

---

## ***Supplementary Material:*** **Experimental Observation of Dissolution Finger Growth in Radial Geometry**

L Xu\*, P Szymczak, R Toussaint, EG Flekkøy and KJ Måløy

\*Correspondence:

Le Xu:

le.xu@fys.uio.no

### **1 SUPPLEMENTAL DATA FOR A REPEATED EXPERIMENT**

This supplemental data gives results from a repeated experiment under the same experimental conditions as described in the main part of manuscript.

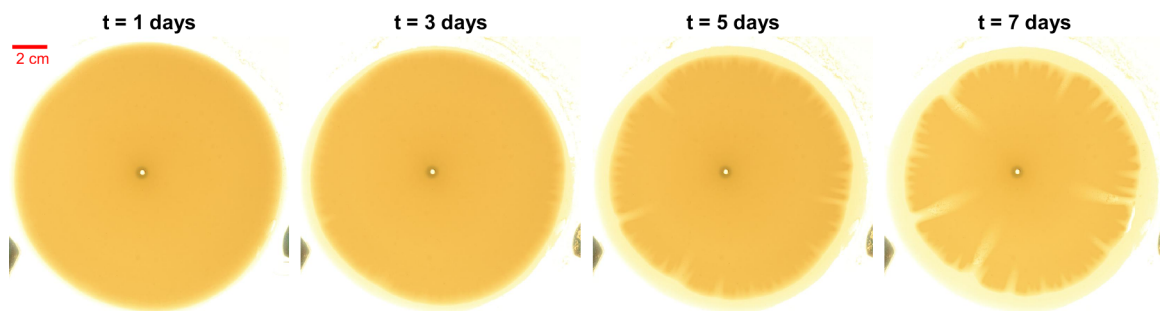


**Figure S1.** Experimental photos of the developing fingering pattern at different moments of time. The time interval between the photos is 2 days. In the circular plaster sample, the dark yellow disk is the undissolved part of plaster and the light yellow part represents the dissolved or partially dissolved part.

## Dissolution Front Propagation with Time

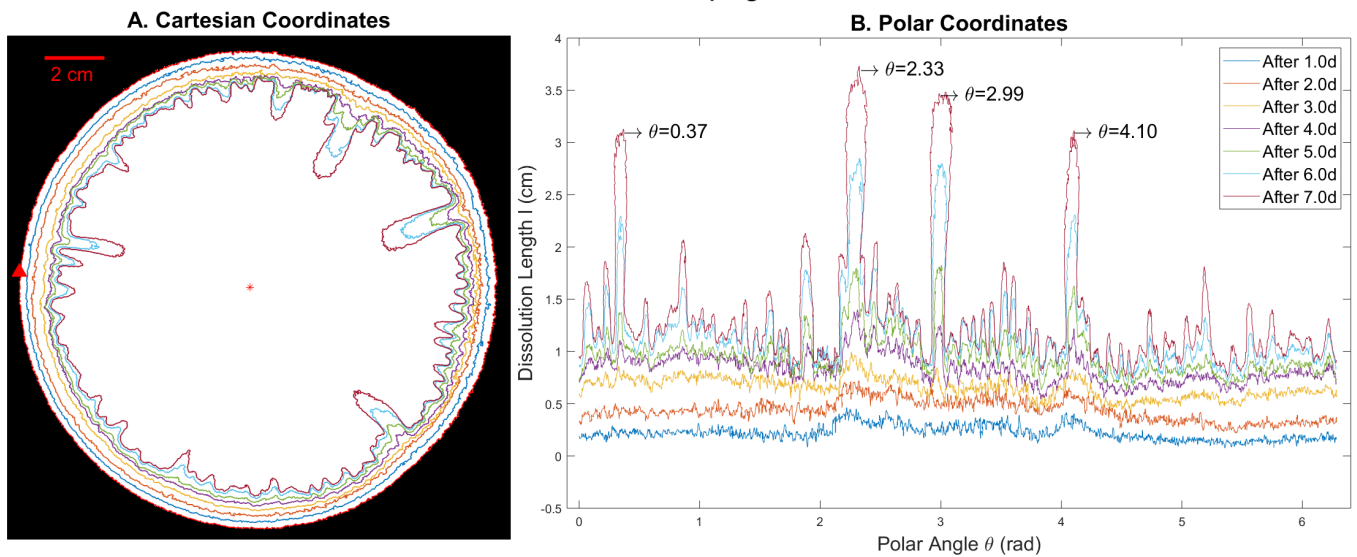


**Figure S2.** Fig.A: Dissolution front propagation with time in Cartesian coordinates. The outermost red circle is the initial boundary, the red star marks the origin, where the outlet is located. The red arrow shows the point where  $\theta = 0$  and the direction in which the polar angle increases. Different colors of the curves show the dissolution front in different times with the time interval of 1 day between two neighboring curves. Fig.B: The evolution of the dissolution length with time is shown in polar coordinates, obtained by calculating  $l(\theta, t) = D(\theta, t = 0) - D(\theta, t)$  from binary experimental images. Different colors represent different times corresponding to the colors in Fig.A. The longest finger located at  $\theta = 2.33$  radians and three second longest fingers located at  $\theta = 0.37$ ,  $\theta = 2.99$  and  $\theta = 4.10$  radians, as indicated in the plot.

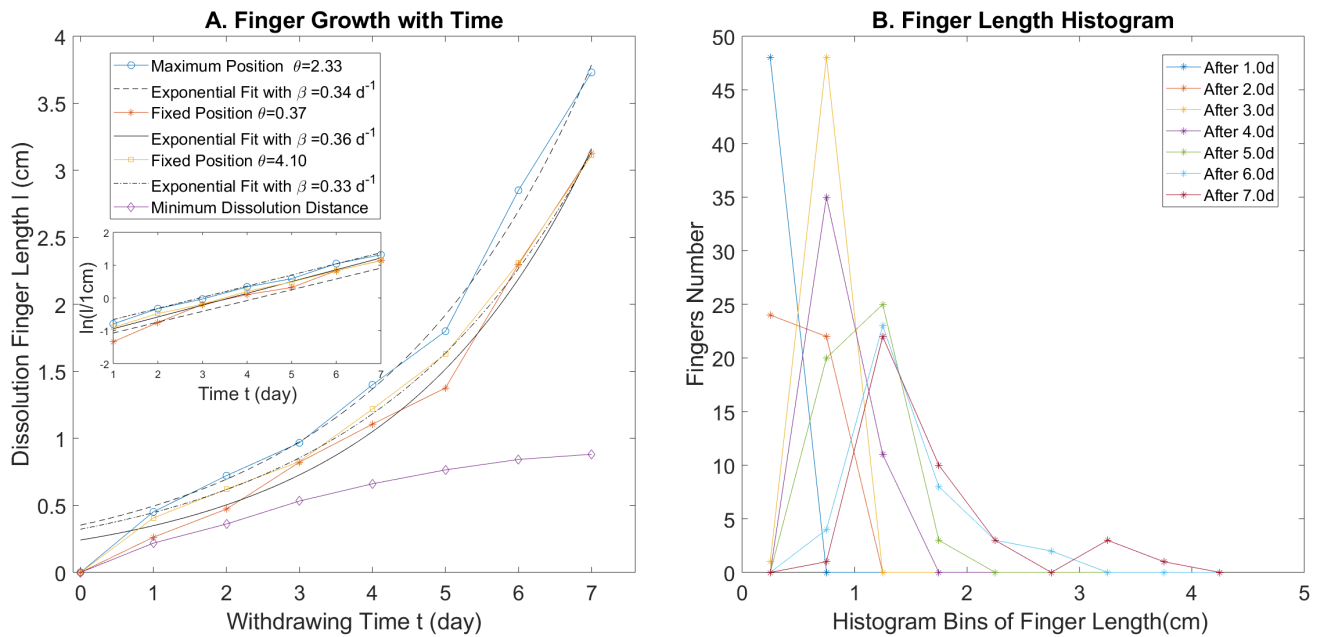


**Figure S3.** Fig A: The finger length evolution with time. The longest and two second longest fingers growth with time are displayed. Fingers located at different angular positions (see Fig.S2 B) are represented by different colors. The finger growth with time at these positions (fixed  $\theta$ ) have been fitted with an exponential function  $l = a \cdot e^{\beta t}$ , displayed by black curves (solid or dashed). Minimum dissolution distance evolution is shown by the purple curve. The inset shows the exponential fits for the finger length vs time. Fig B: Dissolution finger length histograms obtained by counting the peaks in the dissolution length profiles (see Fig.S2.B). Different colors represent different times. The histogram bins cover the range 0 to 4.5 cm with bin size 0.5 cm.

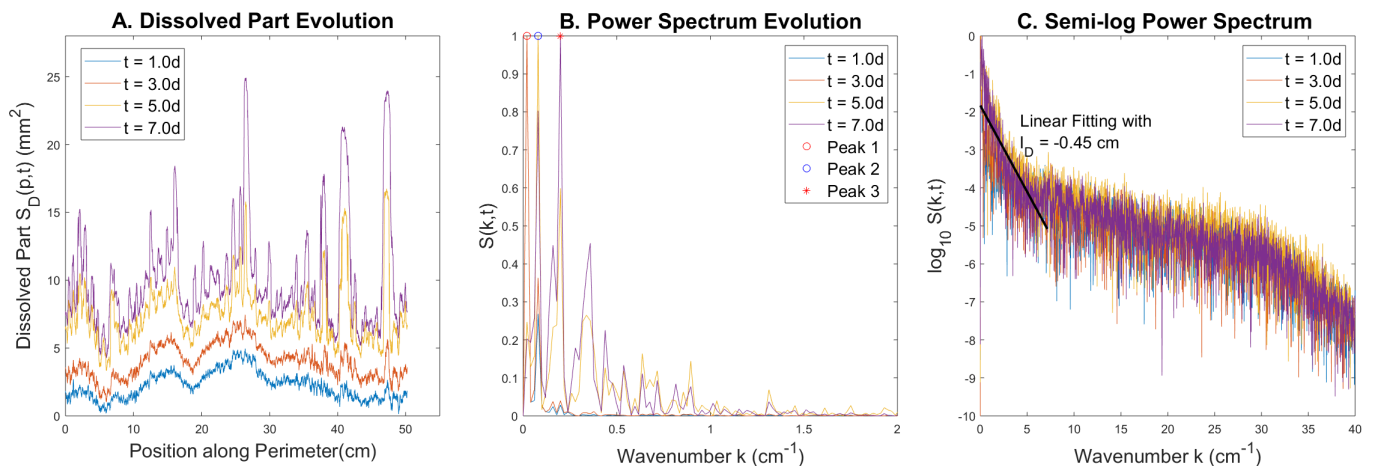


**Figure S4.** A: The local dissolved part  $S_D(p, t)$  at different time moments. B: The power spectrum of  $S_D(p, t)$  profiles presented in panel A. Three main peaks are indicated in the plot. The first two (marked by red and blue circles) are related to the initial geometry of the plaster sample. On the other hand, the peak at  $0.20 \text{ cm}^{-1}$  with wavelength  $\sim 5 \text{ cm}$  (marked by the red star) is related to the characteristic wavelength of the fingering pattern. C: Semi-log plot of the power spectrum, which allows to observe power amplitude trends in a larger scope. The amplitude decays almost exponentially with wavenumber at low wavenumber (high wavelength), followed by a flat plateau at higher wavenumbers. The solid black line in Fig.C is the linear fit, the slope of which gives the characteristic decay length,  $l_D = 0.45 \text{ cm}$ .

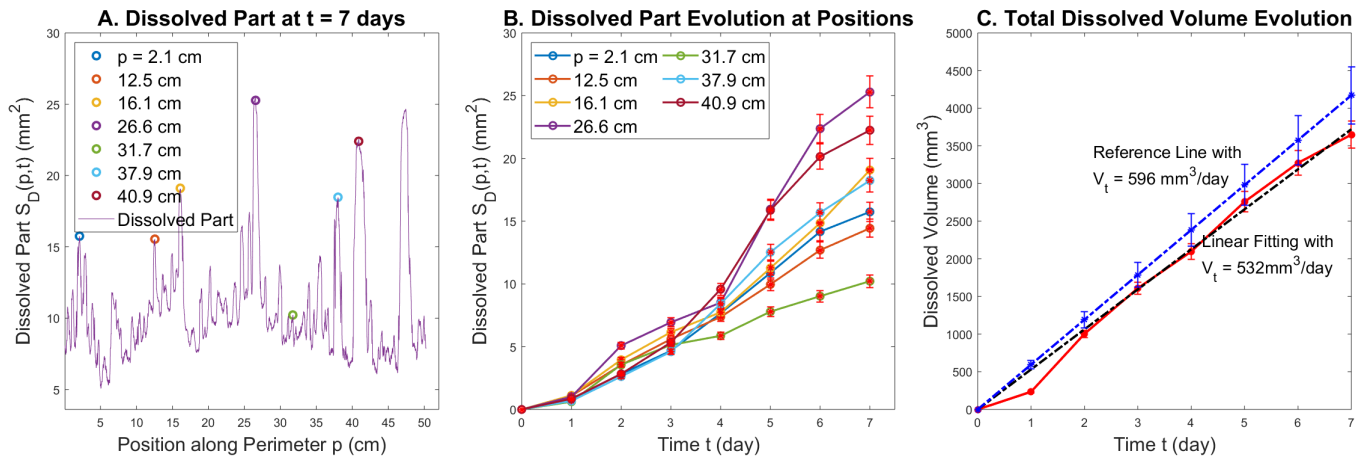


**Figure S5.** The left panel (A) shows the local dissolved part along the perimeter,  $S_D(p, t)$  at  $t = 7$  days. The positions corresponding to the individual fingers, at  $p = [2.1, 12.5, 16.1, 26.6, 31.7, 37.9, 40.9]$ cm are marked with color circles. The centre panel (B) displays the growth of  $S_D(p_i, t)$  at these positions with error bars. The right panel (C) shows the total dissolved volume as a function of time (red line) together with a linear fit (black line) and the theoretical estimate (blue line). The uncertainty of these two lines are displayed with error bars. The overlap between error bars show the experimental measurement fits well with the theoretical estimate.

## 2 PERIODIC PROPERTIES OF THE INITIAL FRONT

This part of supplemental data shows the Fourier spectrum of the boundary of the plaster sample at the beginning of the dissolution process. As observed in Figs.S6 and S7, the initial boundary deviates from an ideal circle. In particular, we observe two peaks in FFT power spectrum at low frequencies (long wavelengths).

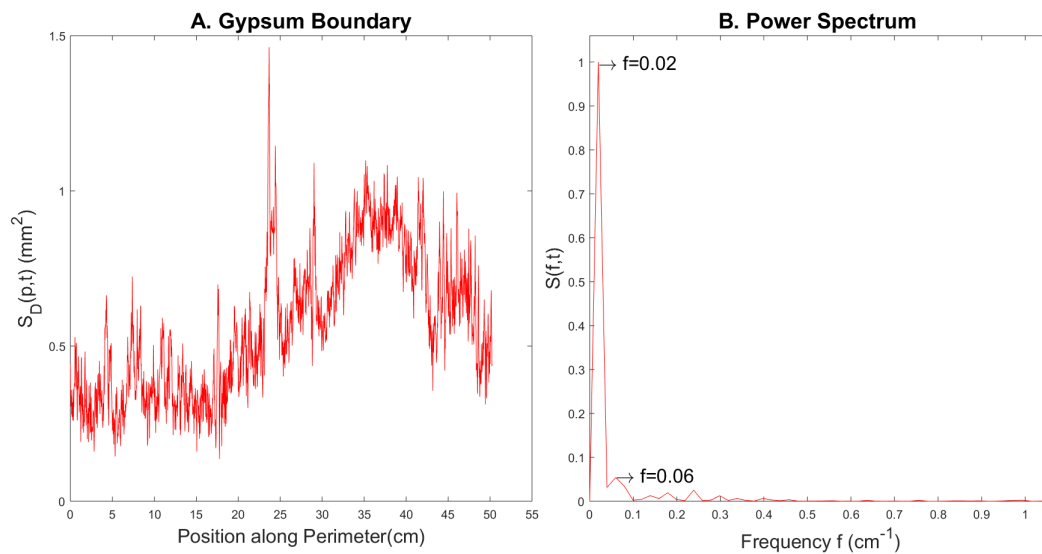


**Figure S6.** Fig A: The initial profile of the outer boundary of the system corresponding to the experiment described in the main text. Fig B: The power spectrum of the signal from panel A, showing two peaks corresponding to long wavelengths.

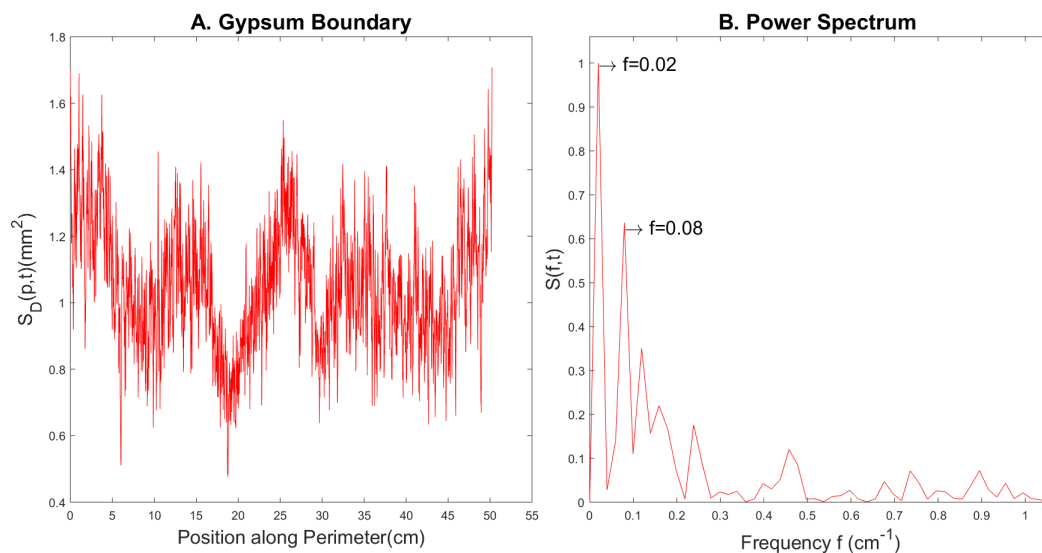


**Figure S7.** Fig A: The initial profile of the outer boundary of the system corresponding to the second, repeated experiment described in the supplementary material. Fig B: The power spectrum of the signal from panel A, showing two peaks corresponding to long wavelengths.